Soft Matter

PAPER

Liquid marble coalescence via vertical collision

Jing Jin, Chin Hong Ooi, Dzung Viet Dao and Nam-Trung Nguyen*

Received 00th January 20xx,
Accepted 00th January 20xx

DOI: 10.1039/x0xx00000x

www.rsc.org/softmatter

The coalescence process of liquid marbles is vital to their promising uses as reactors or mixers in digital microfluidics. However, the underlying mechanisms and critical conditions of liquid marble coalescence are not well understood. This paper studies the coalescence process of two equally-sized liquid marbles via vertical collision aided by dielectrophoretic handling. A liquid marble was picked up using the dielectrophoretic force and then dropped vertically onto another liquid marble resting on a hydrophobic powder bed. The whole collision process was recorded by a high-speed camera and the recorded images were then analysed to derive the generalised boundary conditions of liquid marble coalescence. By varying the marble volume, impact velocity and offset ratio in the experiments, we conclude that liquid marble coalescence can occur through the coating pore opening mechanism. We quantitatively meaured the radius change versus time of liquid neck formed between two coalescing marbles and estimated the maximum deformation of impacting marbles before rupture in rebound cases. We also qualitatively described the redistribution of coating particles at the impact area during coalescence as well as the consequent ejection of particles. Finally, we summarised the critical conditions for liquid marble coalescence, providing a frame for future applications involving liquid marbles as micromixers and microreactors.

Introduction

A liquid marble (LM) is a small liquid droplet coated with multiple layers of nano/microparticles. Most of these coating particles are hydrophobic, allowing a LM to be manipulated like a soft solid.[1-6] As a competitive alternative to superhydrophobic surfaces, LMs exhibit a non-wetting property on various solid and liquid surfaces without the need of surface modification. The porous protective coating physically isolates the liquid core from its surroundings but allows the exchange of gas or vapour. When two LMs are placed in contact, they do not coalesce naturally, even though they are pressed against each other. The pronounced elastic property of LMs enables them to sustain a completely reversible deformation of up to 30%.[7-9] However, LM coalescence is one of the most essential manipulation schemes to realise microfluidic functions such as microreaction and micromixing in digital microfluidics.[10]

A number of coalescence techniques for LMs have been reported in last two decades. Dorvee et al. first reported that two liquid droplets encapsulated by magnetic amphiphilic particles can be manipulated using a magnet and coalesce to perform a reaction.[11] The authors argued that the coalescence process could be aided by increasing the rate at which the two droplets collided. Planchette et al. used a simple set-up to test the robustness of LMs under impact, where a LM was dropped freely onto another much larger one.[12] The results identified a threshold velocity for coalescence and collated it with marble properties such as diameter and particle size. During the collision, both LMs deformed and created a hole of a critical size on each coating. The liquid contents inside then came into contact with each other and the coalescence of LMs could be initiated. The collision converts the kinetic energy accumulated in the falling motion into viscous dissipation energy during coalescence and enables it to work against with the surface deformation and the capillary attractive force among coating particles. Apart from LM coalescence resulted from impact, other coalescence techniques have also been developed. For instance, Bormashenko et al. directly altered the interface between two LMs using a plasma-hydrophilised glass rod, resulting in the forced coalescence of LMs.[13] A LM with a magnetic coating or consisting of a magnetic solution could be accurately positioned and moved across diverse solid and liquid surfaces under the effect of a magnetic field.[14-21] The magnetic force can open the coatings of magnetic LMs and initiate coalescence. In addition, Liu et al. applied a sufficiently high DC voltage to induce the coalescence of two contacting LMs.[22] The threshold voltage of the electro-coalescence process depends strongly on the property of coating particles as well as the surface tension of the liquid core. The authors further demonstrated that multiple marbles in a chain could be driven to merge by higher DC voltages.

Recently, LMs have attracted great attention for their use as microbioreactors for three-dimensional cell culture.[23-28] Due to the small volume of LMs, the miniaturized biological processes in these microbioreactors have several prominent advantages such as the reduced use of reagents and solvents, precisely controlled reaction conditions and greatly shortened reaction time. For this application, solutions such as culture media and cell mixtures need to be added

[a] *Queensland Micro- and Nanotechnology Centre, Griffith University, Brisbane, Queensland 4111, Australia. E-mail: nam-trung.nguyen@griffith.edu.au.*

† Footnotes relating to the title and/or authors should appear here.
Electronic Supplementary Information (ESI) available: [details of any supplementary information available should be included here]. See DOI: 10.1039/x0xx00000x

and mixed in vitro easily, which inevitably involves the coalescence of LMs containing different contents or ingredients. Consequently, a convenient, cost-effective and consistent coalescence technique is the key to the wide application of this LM-based microfluidic platform. The objective of our present work is to systematically study the coalescence process of two LMs via vertical collision using dielectrophoretic picking and placement. We investigate the effects of the marble volume, impact velocity and offset ratio of LMs on coalescence experimentally. We aim to characterise the coalescence mechanism and establish the generalized boundary conditions for a successful LM coalescence event.

Materials and methods

Preparation of liquid marbles for vertical collision

Previous studies on marble collision mainly focused on the impact of a single LM onto solid surfaces as well as the effects of the coating particle size and impact velocity of LMs on different collision outcomes.[29, 30] In this paper, we are only interested in establishing a series of practical operation conditions of coalescence and the coalescence mechanism itself. Therefore, there is no need to compare the effects of the type of coating powder and its particle size on LM coalescence. We thus use only one type of hydrophobic coating powder and fabricate LMs through the widely used conventional rolling method[1-5, 31] that may produce a random aggregate of particles. Furthermore, we select LM pairs with the same volume for the investigation.

LMs were prepared simply by rolling a deionized (DI) water droplet (resistivity of 1.8 × 10^5 Ω·m) on a powder bed of polytetrafluoroethylene (PTFE) (Sigma-Aldrich, nominal diameter of 1 µm) until the droplet was coated as fully as possible, which enables LMs to have a complicated surface structure consisting of multilayer particles. The optical micrographs of PTFE coating took from a top view were shown in Fig. S1, ESI† and the coverage rate of coating particles on the droplet surface is estimated at roughly 90%.[32] Droplet volumes of 5, 10, 15, 20 and 25 µL were dispensed using a micropipette (Thermo Scientific Finnpipette 4500, dispensed volume range from 0.5 to 10 µL). There are several reasons for the volume setting. First, the liquid inside small-volume LMs evaporates greatly before collision. It is also hard to precisely control the marbles smaller than 5 µL for vertical collision. And, more importantly, the strong surface tension effect (the Bond number is much smaller than 1) keeps small marbles elastic and intact upon impact. Besides, due to the unavoidable limitation of experimental solutions, it is impossible to manipulate oversized LMs for vertical collision under the condition that the marbles keep intact. As the thickness of PTFE coating is evidently much smaller than the radius of the DI water droplet, the marble volume was considered the same as that of the corresponding bare droplet. Two identical marbles were created at the same time and manipulated under the same laboratory environment (temperature of 22.5 ± 1 °C and relative humidity of 55 ± 5%) in all experiments.

Experimental set-up

Figure 1 depicts the experimental set-up for LM vertical collision, which comprises of a polymethyl methacrylate (PMMA) holder with an electrode, an *x-y-z* linear stage, a high-voltage converter, a custom-made automatic triggering device, a benchtop power supply and a high-speed camera. The holder was made of 10 mm thick PMMA plates and has a through hole with 0.8 mm diameter to carry a cylindrical stainless steel electrode of the same diameter. The *x-y-z* linear stage consists of a programmable *x-y* linear stage (Zaber Technologies T-LS28M, travel range of 28 mm) and a manual linear translation stage (Thorlabs PT1, travel range of 25 mm). The manual linear translation stage was connected to the electrode holder and enabled it to move along the *z* direction. The dielectrophoretic picking and placement relied on a high-voltage DC-DC converter (Eastern Voltage Research HVPS 2) driven by a benchtop power supply (Keithley 2200-30-5, maximum voltage/current of 30 V/5 A). A high-speed camera (Photron Fastcam SA3) was used to record the side view of LM collision events. Video recordings were conducted at a constant rate of 3000 frames per second (fps) with two image sizes, namely 256 × 768 pixels for 5 µL LMs and 512 × 768 pixels for other LMs. The custom-made automatic triggering device connecting the power supply and the high-speed camera started video recording simultaneously with LM release by cutting off the power supply. The recorded images were then analysed using ImageJ (National Institutes of Health, USA).

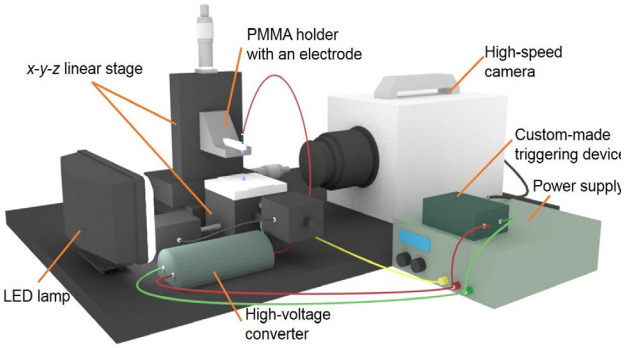

Fig. 1 Schematic of the experimental set-up for LM vertical collision.

Vertical collision of liquid marbles aided by dielectrophoresis

To start with, the two prepared LMs were transported from the PTFE powder bed using a stainless steel chemical spoon and then placed on a glass slide coated with the same PTFE powder. One LM was picked by the dielectrophoretic force produced in the non-uniform electric field of the cylindrical stainless steel electrode. The required input voltage of the DC-DC converter for 5, 10, 15, 20 and 25 µL LMs were 1.25, 1.30, 1.30, 1.35 and 1.40 V respectively. To avoid rupture, the LMs contacted the PTFE layer directly before collision. The images showing the dielectrophoretic picking and release of LMs were given in Fig. S2, ESI†. We can clearly see that the marbles were deformed when picked by the dielectrophoretic force and restored to the initial shape after release. In this paper, the dielectrophoretic picking and placement technique is only used for manipulating LMs to induce vertical collision. The working principle and experimental parameters of this technique will be reported in detail in another separate paper. The other LM with the same size was moved to the position directly below the upper marble through the translational motion of the *x-y* linear stage. By observing the real-time image of

the high-speed camera, the bottom LM was adjusted to different positions, corresponding to three groups of offset ratios between two colliding LMs, namely 0 (head-on collision), 0.4 and 0.8 (oblique collisions).

The offset ratio (X^*) is defined as the dimensionless ratio of the distance between the centres of mass of two LMs (X) to the diameter of the undeformed LM (D) with a tolerance up to 5%, as shown in Fig. 2. Then the upper marble was lifted by the z-axis manual stage to three different heights to produce three corresponding impact velocities of the vertical collision, namely 0.333, 0.386 and 0.438 m/s. In this study, the impact velocity (v) was determined as the average velocity just prior to collision. To reduce the measurement error, we measured the change of position (Δz) of the falling marble in the last three frames prior to collision and divided it by the corresponding time duration (Δt = 3 frames/3000 fps = 0.001 s), namely $v = \Delta z/\Delta t$. These impact velocities were decided by both the necessary experimental conditions for a successful marble coalescence event and the operating limit of linear motion stages. Finally, the upper marble was released to collide with the bottom marble after turning off the electric field. This dielectrophoretic method practically minimises the horizontal velocity of the falling marble to zero so that the rotation and positioning problems of the upper LM during vertical collision can be avoided. Each experimental group with its specific parameters was repeated for at least ten times to reduce contingency. The influence of air on the coalescence process was negligible and thus the upper marble could collide with the bottom marble along a straight path. All the data were collected and compared systematically based on image analysis with ImageJ.

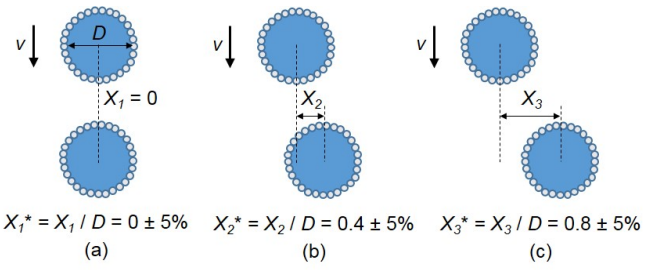

Fig. 2 Schematic of vertical collision of two identical LMs with different offset ratios. (a) Head-on collision (offset ratio X_1^* = 0 ± 5%). (b) Oblique collision (offset ratio X_2^* = 0.4 ± 5%). (c) Oblique collision (offset ratio X_3^* = 0.8 ± 5%).

Theoretical background

We use a simple energy relationship to estimate the coalescence condition of LMs. We assume that two near-spherical LMs (LM 1 and LM 2), which have the same diameter D, collide with each other vertically and merge into a larger coalesced LM (LM 3), as shown in Fig. 3. The coalescence is caused by the energy transformed from the kinetic energy overcoming the surface energy of an individual LM, which results in the particle motion and subsequently liquid-liquid contact on the interface of two colliding LMs. The dimensionless number representing the relative relationship between the kinetic energy and surface energy is the Weber number (We):

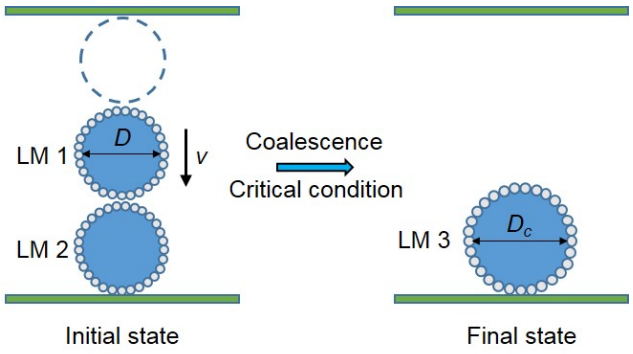

Fig. 3 Schematic of different states of LMs before and after coalescence through vertical collision.

$$We = \frac{\rho D v^2}{\sigma} \quad (1)$$

where ρ, σ, D and v are the effective density, surface tension, diameter and the instantaneous velocity just prior to coalescence of the individual LM respectively. For the convenience of later analysis, we use the modified Weber number (We^*) that is the direct ratio between the kinetic energy $E_k = \pi\rho D^3 v^2/12$ and the surface energy $E_s = \pi D^2\sigma$ of the individual LM:

$$We^* = \frac{E_k}{E_s} = \frac{1}{12}\frac{\rho D v^2}{\sigma} = \frac{1}{12}\mathrm{We} \quad (2)$$

We first select LM 1 as the analysis objective. LM 1 is released from attaching to the sample holder. The falling process is regarded as the free-fall motion, neglecting the viscous loss of air due to the small travelling distance. The kinetic energy of the impact can be therefore adjusted with the initial height of LM 1:

$$E_k = \frac{\pi\rho D^3 v^2}{12} = \frac{\pi\rho D^3}{6} gh \quad (3)$$

where g is the gravitational acceleration, and h is the initial height of LM 1. After coalescence, the volume of the coalesced LM (LM 3) is the sum of the two initial LMs (LM 1 and LM 2), thus its diameter can be estimated as $D_c = 2^{1/3}D$. The energy balance between the states before and after coalescence is:

$$2E_s + E_k = E_{s,c} + E_{\mathrm{loss}} \quad (4)$$

where $E_{s,c} = \pi {D_c}^2\sigma$ is the surface energy of the coalesced LM and E_{loss} is the energy expended to break the interface between the initial individual LMs. Equation (4) can be written as:

$$2\pi D^2\sigma + \frac{\pi\rho D^3 v^2}{12} = 2^{2/3}\pi D^2\sigma + E_{\mathrm{loss}} \quad (5)$$

Rearranging the equation (5) above for the ratio between the energy loss and initial surface energy results in:

$$\frac{E_{\mathrm{loss}}}{\pi D^2\sigma} = We^* + 0.413 \quad (6)$$

For coalescence to occur, the energy loss should be at least more than the initial surface energy of an individual LM (LM1 or LM2), namely $\frac{E_{\mathrm{loss}}}{\pi D^2\sigma} > 1$. Thus we can derive a critical modified Weber number as the boundary condition for LM coalescence:

$$\mathrm{We_c}^* = 1 - 0.413 = 0.587 \approx 0.6 \quad (7)$$

This means the kinetic energy of the individual LM should be at least around 60% of its initial surface energy to make coalescence happen.

Results and discussion

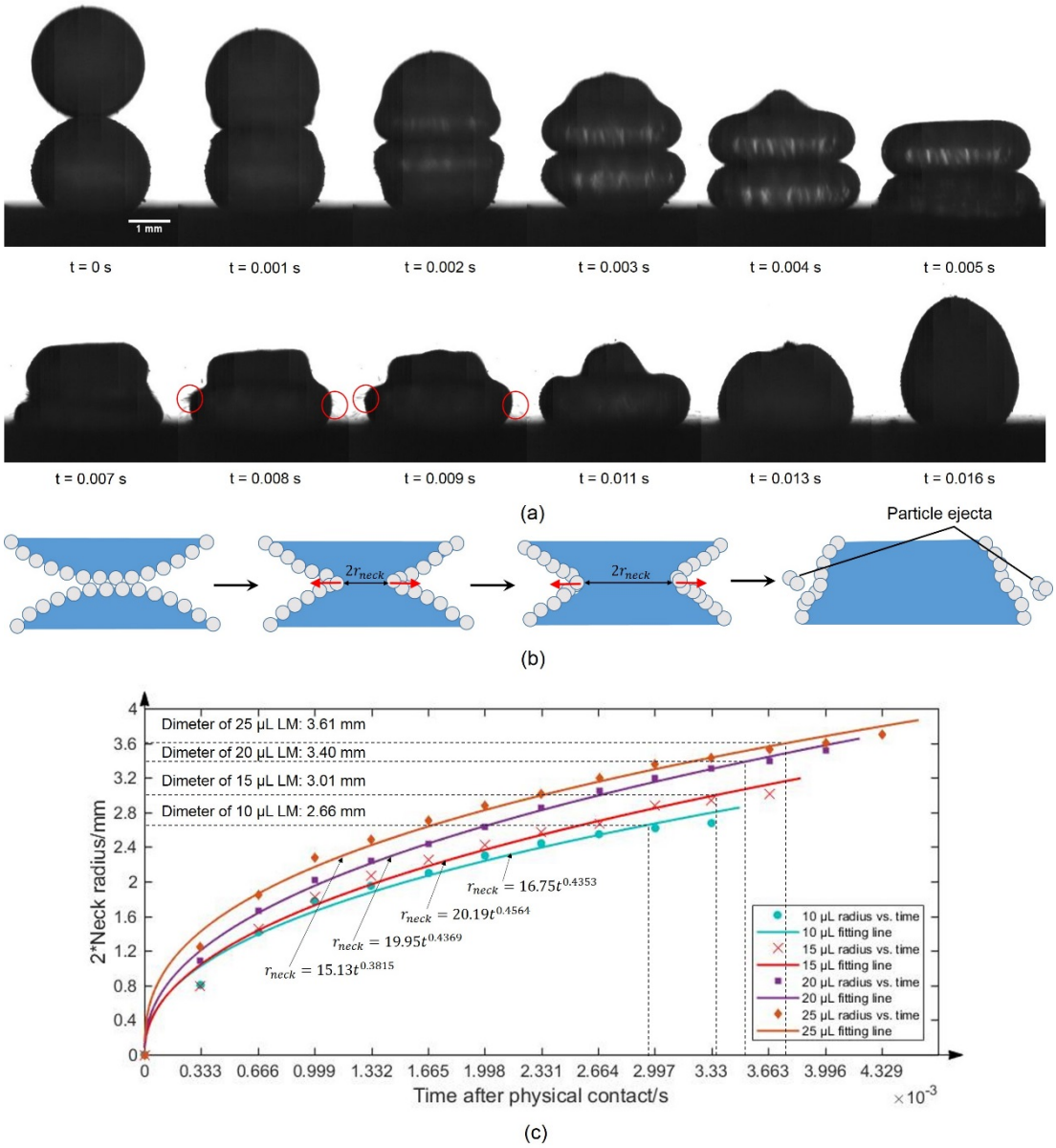

Fig. 4 (a) Image sequence of the coalescence process of two 10 μL LMs via head-on collision (impact velocity of 0.438 m/s). The start point was set to the moment that two LMs just contacted with each other (t = 0 s). The red circles show the areas that the particle ejecta appeared. (b) Schematic of the particle motion on protective coatings and neck growth during coalescence. The red arrows imply the outward particle motion direction. (c) The growth trend of liquid radius versus time between two coalescing LMs in the head-on collision with an impact velocity of 0.438 m/s.

Outcomes of liquid marble vertical collision

Generally, there were two outcomes of LM vertical collision, namely coalescence and rebound (Video S1-S10, ESI†). The coalescence process of two equally-sized LMs is discussed first. As mentioned above, an upper marble fell down freely after removing the dielectrophoretic force. During the falling motion, a part of the gravitational potential energy of the upper marble converted to its kinetic energy according to the energy conservation law, enabling this marble to have an initial velocity before collision. The impact velocity was measured from the last three frames prior to collision as the method described above. When the upper marble collided with the sessile bottom marble, the external PTFE coating layers contacted with each other first (Fig. 4(a), t = 0 s). Both LMs deformed symmetrically due to the released kinetic energy (Fig. 4(a), t = 0.001-0.005 s). Along with the marble deformation, the hydrophobic coating particles near the contact area flowed rapidly to the periphery of the two LMs due to the fluid flow inside marbles. Then bare liquid regions were exposed on the interface, leading to the occurrence of liquid-liquid contact. There were some cracks formed on the particle shells, which effectively proves the direct liquid-liquid contact between two coalescing LMs, as shown in Fig. S3, ESI†. A liquid neck with a meniscus shape between the two coalescing LMs

nucleated and grew rapidly. Once the neck radius increased to the radius of the corresponding individual LM, the two colliding LMs would totally merge into a whole larger marble. Simultaneously, the coating particles aggregated on the surface and became overcrowded after coalescence, as depicted in Fig. 4(b). The overcrowding of these particles gave rise to the ejection of surplus particles at impact area, as highlighted by red circles in Fig. 4(a) (t = 0.008-0.009 s). In order to better understand the dynamics of LM coalescence, we quantitatively measured the neck radius change versus time in head-on coalescence cases with an impact velocity of 0.438 m/s and fitted the data points using Curve Fitting Tool in Matlab (Fig. 4(c)). It is clear to see that the radius of liquid neck increased with time following a certain power scaling law with a power exponent ranging from 0.3815 to 0.4564, namely $r_{neck} \propto t^{0.3815\sim0.4564}$, which is similar to the coalescence behaviour of bare droplets.[10, 33-37] After coalescence, the merged LM oscillated and slowly evolved to its equilibrium shape. However, the relaxation process of the merged LM will not be discussed in this paper.

Another important vertical collision outcome for two equally-sized LMs is rebound. In the rebound process, the first half period (Fig. 5(a), t = 0-0.004 s) was reversible deformation, where both the upper marble and bottom marble experienced a large deformation while the coating layers kept intact. We quantitatively measured the maximum deformation of LMs upon head-on impact and chartered it with the aspect ratio of the bottom LM (Fig. 5(b)). The initial aspect ratio (D_0/h_0) of 5 µL LMs is about 1.13 and increases to 3.76 after the head-on collision with an impact velocity of 0.438 m/s. For 10 and 15 µL LMs, the initial aspect ratios are 1.20 and 1.27 respectively and the maximum aspect ratios (D_{max}/h_{min}) for rebound cases with an impact velocity of 0.333 m/s are 3.13 and 3.14 respectively, which indicates that the maximum deformation of 10 and 15 µL LMs in rebound cases has the same order of magnitude. It is noticeably that there was no rebound event occurred in head-on collision for 20 and 25 µL even with the lowest impact velocity. However, as the deformation reached its maximum extent, all the kinetic energy of the upper marble was restored into the surface energy of the two stationary marbles, and then the remaining kinetic energy caused the marbles to bounce off. The rebound process happened because the kinetic energy of the upper marble stored in the falling motion did not meet the energy need for breaking the particle layers between the two marbles. The excellent elastic property of LMs resulting from the porous protective coating enabled them to bounce off each other. As the LMs moved away from the impact area, the LMs recovered to their initial shapes without any leakage (Fig. 5(a), t = 0.021 s).

Effect of marble volume on liquid marble collision outcomes

In this study, the volume of LM was varied from 5, 10, 15, 20 to 25 µL. These volumes are the most common used ones in chemical and biological assays. The contour plots in Fig. 6 clearly show that the coalescence and rebound processes both appeared in the vertical collision of LMs with different volumes. In general, LMs with larger volumes were much easier to coalesce after falling down from a given height as compared with the counterparts with smaller volumes. We use coalescence rate (Ω) to imply the ratio of coalescence cases in 10 trials of each experimental group.

For the collision of 5 µL LMs, the coalescence rate was no more than 50% in all experimental groups except for the oblique collision of 5 µL LMs with an offset ratio of 0.4 and an impact velocity 0.438 m/s (Ω = 80%). This is because the excellent elasticity of small marbles resulting from the strong surface tension effect enabled them to bounce off to release all the kinetic energy (Fig. S4 and Table S1, ESI†). As for the collision of 10 µL LMs, coalescence was much easier to occur with larger deformation because of the decrease of Laplace pressure due to volume increase, especially in head-on collisions with impact velocities of 0.386 and 0.438 m/s (Ω = 100%). When the marble volume increases to 15, 20 and 25 µL, the corresponding diameter is larger than the capillary length of pure water (2.7 mm), which means these larger volume marbles are

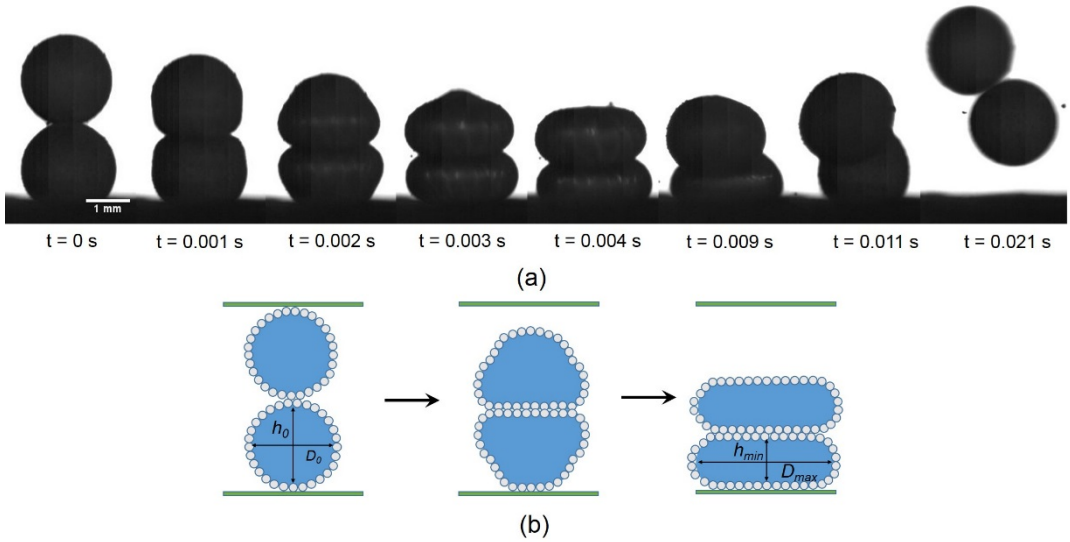

Fig. 5 (a) Image sequence of the rebound process of two 5 µL LMs via head-on collision (impact velocity of 0.438 m/s). The start point was set to the moment that two LMs just contacted with each other (t = 0 s). The red circles show the areas that the particle ejecta appeared. (b) Schematic of the maximum deformation (D_{max}/h_{min}) of the bottom LM during vertical impact in rebound cases.

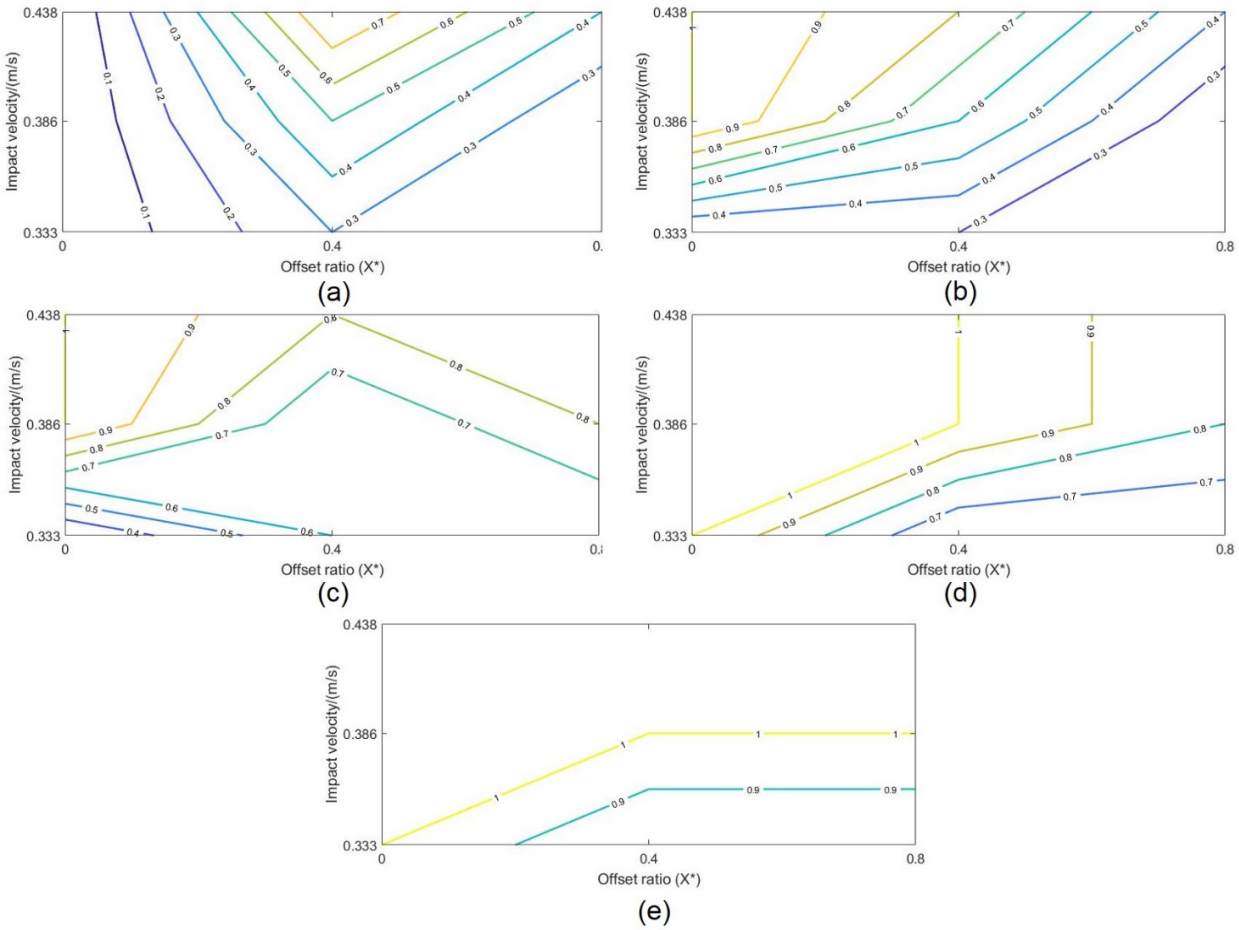

Fig. 6 The contour plots for coalescence rate of LM collision. (a) 5 μL LMs. (b) 10 μL LMs. (c) 15 μL LMs. (d) 20 μL LMs. (e) 25 μL LMs.

subject to more gravitational deformation in vertical collision. Thus the occurrence rate of coalescence event was almost no less than 60% in these impact experiments. In some cases, for example, head-on collisions of 15, 20 and 25 μL LMs with impact velocities of 0.386 and 0.438 m/s and oblique collisions of 20 and 25 μL LMs with an offset ratio of 0.4 when the impact velocity was no lower than 0.386 m/s, only coalescence occurred. The coating particles that could not provide a good cover to the liquid core inside 15, 20 and 25 μL LMs upon impact. The cracks were easily to form on the interface and gave rise to direct liquid-liquid contact, resulting in marble coalescence. Besides, the larger volume of LMs provides more kinetic energy to the upper marble after travelling the same distance as the 5 μL LM, which is also beneficial for losing marble integrity.

Effect of offset ratio on liquid marble collision outcomes

For 5 μL LM collision, coalescence tended to happen in oblique collisions regardless of the impact velocity ($\Omega \geq 20\%$), especially in the oblique collision with an offset ratio of 0.4 and an impact velocity 0.438 m/s, as indicated by Fig. 6(a). In the head-on collision process of 5 μL LMs, the kinetic energy of upper LM was not enough to break down the powder layers between two individual LMs. The protective coatings greatly improved the integrity of these 5 μL LMs, isolating the small-volume liquid cores from contacting each other. The prominent elasticity of these LMs enabled them to bounce off. By contrast, in the oblique collision of 5 μL LMs with an offset ratio of 0.4, the shearing effect also played an important role except for the kinetic energy in the rupture of protective coatings, as highlighted by red arrows in Fig. 7(a). The shear stress produced in the off-centre collision of two LMs partly promoted the particle motion along the tangent direction in PTFE powder layers and let the liquid cores inside contact each other much quicker. We used the geometrical relationship of two colliding LMs with different offset ratios to calculate the shear rate between them, as shown in Figs. S5&S6 and Table S2, ESI†. When the offset ratio increased to 0.8 in the oblique collision of 5 μL LMs, the compression force between two impacting LMs greatly reduced and the contact time shortened a lot although the shear stress still facilitated the particle motion in local areas of the interface. Thus a successful LM coalescence event was harder to achieve at the same impact velocity.

However, for 10, 15, 20 and 25 μL LM collisions, coalescence tended to occur in head-on collision, especially in head-on collisions with impact velocities of 0.386 and 0.438 m/s ($\Omega \approx 100\%$), as indicated by Fig. 6(b)-(e). The head-on collision ensured all the kinetic energy are converted to the energy for deformation dissipation of two LMs, as shown in Fig. 7(b). Therefore, the rupture of protective coatings was easy to happen when the impact velocity was no lower than 0.386 m/s. In terms of 10, 15, 20 and 25 μL LM oblique collisions, the shear rate of larger marble decreased considerably (Table S2, ESI†) and due to the large surface area of two impacting LMs, the

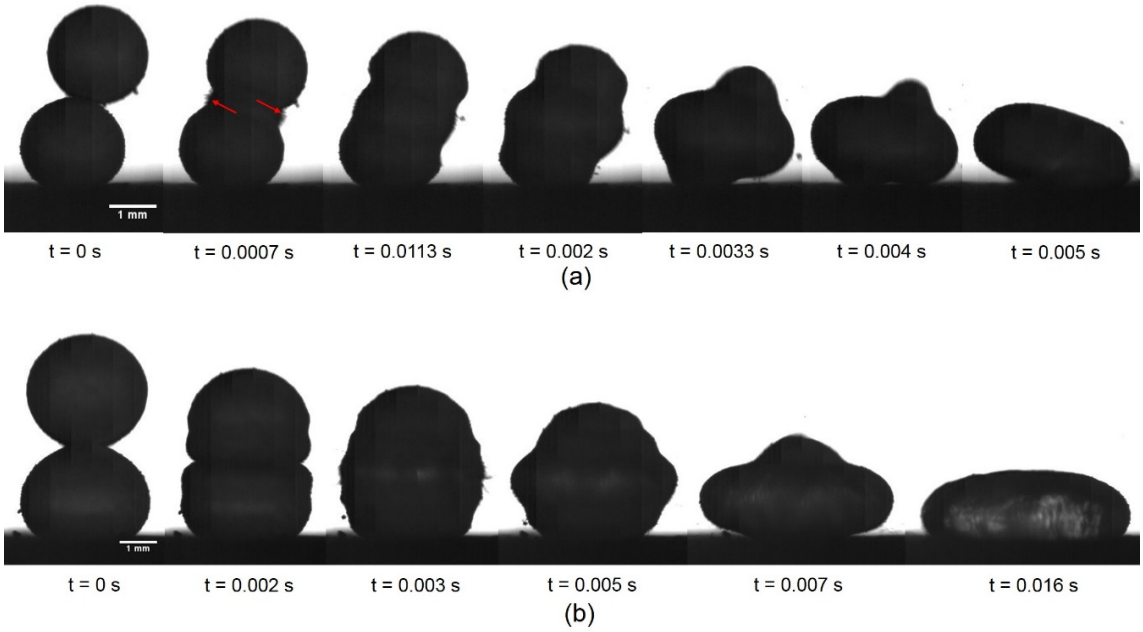

Fig. 7 (a) Image sequence of the coalescence process of two 5 μL LMs via oblique collision (offset ratio of 0.4, impact velocity of 0.333 m/s). The red arrows imply the force direction of shear stress. (b) Image sequence of the coalescence process of two 20 μL LMs via head-on collision (impact velocity of 0.438 m/s). The start point was set to the moment that two LMs just contacted with each other in both groups of images.

shearing effect was not obvious. Thus the coalescence process of LMs appeared less than its counterparts in head-on collisions for 10, 15, 20 and 25 μL LMs. Particularly, 10 μL LMs tended to bounce off in oblique collision with an offset ratio of 0.8 when the impact velocity was small, which needs further investigation. The coalescence rate of 15 μL LM collision decreased to 60% when the offset ratio increased to 0.4 and did not change much by increasing the offset ratio further to 0.8. For the collisions of 20 and 25 μL LMs with high impact velocities, only coalescence event occurred when the offset ratio was no larger than 0.4 and coalescence still dominated over rebound in oblique collisions with an offset ratio of 0.8.

Effect of impact velocity on liquid marble collision outcomes

In general, the larger the impact velocity is, the more occurrence rate is coalescence event. According to the energy conservation law, the longer the falling distance is, the larger the impact velocity is. Therefore, more kinetic energy is available for dissipating into LM deformation and breaking the protective layers of LMs. The kinetic energy of an individual LM should be at least around 60% of its initial surface energy to make coalescence happen according to our theoretical estimation. However, it is not true for the head-on collision of 5 μL LMs, where only the rebound event occurred with all impact velocities. In the case of head-on collisions of 10, 15, 20 and 25 μL LMs, both higher impact velocities, namely 0.386 and 0.438 m/s, enabled the coalescence events. There were less coalescence events for 10 and 15 μL LMs when the impact velocity decreased to 0.333 m/s (Ω = 40%). However, 20 and 25 μL LMs still coalesced at this smallest impact velocity. When it turns to oblique collisions with other two groups of offset ratios (0.4 and 0.8), the decrease in impact velocity meant a lower probability of coalescence even the shearing effect played a role in the LM collision process. Increasing offset ratio did not strengthen the effect of shear stress on coalescence although the shear rate increased with the offset ratio. In particular, when the impact velocity decreased to 0.386 m/s in the oblique collision of 10 μL LMs with an offset ratio of 0.8, the main collision outcome was rebound. With larger LM volumes (15, 20 and 25 μL), decreasing impact velocity did not have an obvious effect on the collision outcome, as the marbles still tended to coalesce rather than bounce.

Critical modified Weber number for liquid marble coalescence

Fig.8 shows the trend of the coalescence rate (Ω) versus the modified Weber number (We^*) for all experimental cases in this study. Based on the experimental data, it is clear to see that coalescence was more likely to occur than rebound when We^* was more than 0.581. This experimental critical modified Weber number (We_c^* = 0.581) is in reasonable agreement with the theoretic value (0.587) we estimated above, which indicates the energy-based theory used in this paper goes well with experiments. For the head-on collision of LMs with different volumes, the critical modified Weber number was valid in most cases of the experiments. The coalescence rate was always 100% when We^* was more than We_c^* in head-on collisions. By contrast, the coalescence rate was mostly no more than 30% in head-on collisions with We^* below We_c^*. When increasing the offset ratio in LM collision, the critical modified Weber number was still valid in a certain number of experimental cases. However, coalescence event generally happens earlier in oblique collisions. It is noteworthy that the coalescence rate of oblique collisions with large offset ratios was mostly much higher than that of head-on collisions below the critical modified Weber number. However, the coalescence rate of oblique collisions did not increase dramatically when We^* approaches We_c^*. This means that increasing the offset ratio of vertical collision is not beneficial for high modified Weber number. From all these

descriptions, we argue that the coalescence rate (Ω) is an error function of the critical modified Weber number (We_c*) roughly. We use MATLAB (MathWorks) to fit the data points in Fig. 8 to an error function. The relationship of Ω and We_c* can be fitted as:

$$\Omega = 0.521\,\mathrm{erf}(12.855We^* - 5.461) + 0.470 \quad (8)$$

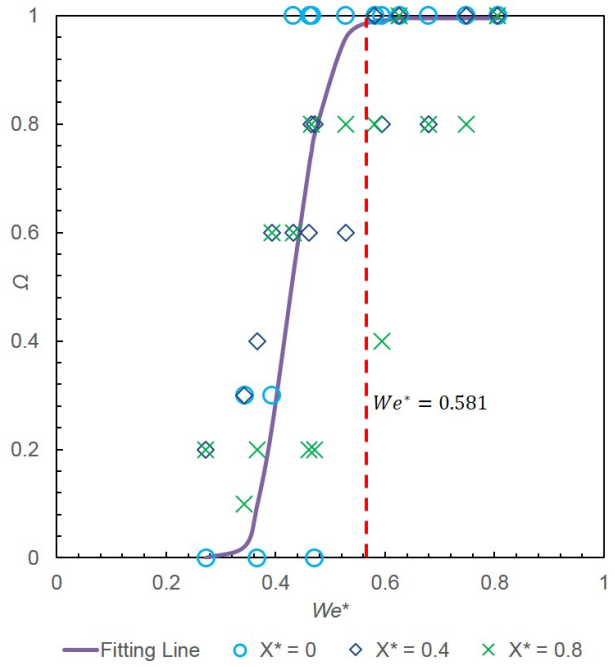

Fig. 8 Coalescence rate (Ω) as a function of modified Weber number (We*) for different dimensionless offset ratios (X*).

Conclusions

This paper experimentally investigated the dynamics of LM coalescence through vertical collision. The vertical collision was implemented by the dielectrophoretic picking and placement using our customised high-voltage device. By varying the marble volume, impact velocity and offset ratio of LMs, coalescence and rebound phenomena both appeared in the vertical collision of LMs with volumes of 5, 10, 15, 20 and 25 µL. When the upper marble collided with the stationary bottom marble with enough kinetic energy, the porous coating layers first contacted each other. Subsequently, the hydrophobic particles on the coating moved rapidly to the periphery of the two water marbles due to the fluid flow inside the marbles. Consequently bare liquid regions appeared on the interface, resulting in direct liquid-liquid contact. Then a liquid neck with a meniscus shape was formed between two coalescing LMs and grew rapidly following a power scaling law. When the radius of liquid neck increased to the dimeter of corresponding LMs, two colliding LMs would merge into a whole larger LM. The overcrowding of coating particles gave rise to the ejection of extra particles around the impact area after coalescence. Generally, LMs with larger volumes were much easier to coalesce when comparing with their counterparts with smaller volumes. For 5 µL LM collision, coalescence tended to occur with oblique collision due to the shear stress produced at the contact area. In head-on collision, the protective coatings consisting of PTFE powders effectively protected the integrity of 5 µL LMs. While for 10, 15, 20 and 25 µL LM collision, coalescence tended to appear in the head-on collision. The head-on collision ensured all the kinetic energy to convert to the energy for deformation dissipation of both LMs. Therefore, the protective coatings could easily break down regardless of the impact velocity. In the cases of oblique collision of 10, 15, 20 and 25 µL LMs, due to the reduced shear rate and the large contact area between two LMs during collision, the shearing effect did not dominate marble collision process. Among the three groups of impact velocities in this study, the larger the impact velocity is, the more occurrence rate is the coalescence event. Therefore, we summarised the critical condition above for LM coalescence, aiming to facilitate a better understanding of future applications involving LMs as micromixers and microreactors.

Conflicts of interest

We have no conflicts to declare.

Acknowledgements

We acknowledge Queensland Micro- and Nanotechnology Centre for providing the facilities to make the experiments possible and the Australian Research Council for the discovery Grant DP170100277. Jing Jin is supported by Griffith University International Postgraduate Research Scholarships (GUIPRS).

References

1. P. Aussillous and D. Quere, *Nature*, 2001, **411**, 924-927.
2. P. Aussillous and D. Quere, *Proceedings of the Royal Society A: Mathematical, Physical and Engineering Sciences*, 2006, **462**, 973-999.
3. P. Aussillous and D. Quere, *JFM*, 2004, **512**.
4. E. Bormashenko, *Current Opinion in Colloid & Interface Science*, 2011, **16**, 266-271.
5. G. McHale and M. I. Newton, *Soft Matter*, 2011, **7**, 5473.
6. C. H. Ooi and N.-T. Nguyen, *Microfluid. Nanofluid.*, 2015, **19**, 483-495.
7. E. Bormashenko, R. Pogreb, R. Balter, H. Aharoni, Y. Bormashenko, R. Grynyov, L. Mashkevych, D. Aurbach and O. Gendelman, *Colloid. Polym. Sci.*, 2015, **293**, 2157-2164.
8. S. Asare-Asher, J. N. Connor and R. Sedev, *J. Colloid Interface Sci.*, 2015, **449**, 341-346.
9. Z. Liu, X. Fu, B. P. Binks and H. C. Shum, *Langmuir*, 2015, **31**, 11236-11242.
10. J. Jin, C. Ooi, D. Dao and N.-T. Nguyen, *Micromachines*, 2017, **8**, 336.
11. J. R. Dorvee, A. M. Derfus, S. N. Bhatia and M. J. Sailor, *Nat Mater*, 2004, **3**, 896-899.
12. C. Planchette, A.-L. Biance, O. Pitois and E. Lorenceau, *Physics of Fluids*, 2013, **25**, 042104.
13. E. Bormashenko, R. Balter, D. Aurbach, A. Starostin, V. Valtsifer and V. Strelnikov, Ariel, Israel, 2014.
14. Y. Xue, H. Wang, Y. Zhao, L. Dai, L. Feng, X. Wang and T. Lin, *Adv. Mater.*, 2010, **22**, 4814-4818.
15. Y. Zhao, J. Fang, H. Wang, X. Wang and T. Lin, *Adv. Mater.*, 2010, **22**, 707-710.

16. Y. Zhao, Z. Xu, H. Niu, X. Wang and T. Lin, *Adv. Funct. Mater.*, 2015, **25**, 437-444.
17. Y. Zhao, Z. Xu, M. Parhizkar, J. Fang, X. Wang and T. Lin, *Microfluid. Nanofluid.*, 2012, **13**, 555-564.
18. M. K. Khaw, C. H. Ooi, F. Mohd-Yasin, R. Vadivelu, J. S. John and N. T. Nguyen, *Lab Chip*, 2016, **16**, 2211-2218.
19. C. H. Ooi, A. V. Nguyen, G. M. Evans, D. V. Dao and N. T. Nguyen, *Sci. Rep.*, 2016, **6**, 38346.
20. L. Zhang, D. Cha and P. Wang, *Adv. Mater.*, 2012, **24**, 4756-4760.
21. E. Bormashenko, R. Pogreb, Y. Bormashenko, A. Musin and T. Stein, *Langmuir*, 2008, **24**, 12119-12122.
22. Z. Liu, X. Fu, B. P. Binks and H. C. Shum, *Soft Matter*, 2017, **13**, 119-124.
23. T. Arbatan, A. Al-Abboodi, F. Sarvi, P. P. Chan and W. Shen, *Adv. Healthc. Mater.*, 2012, **1**, 467-469.
24. F. Sarvi, K. Jain, T. Arbatan, P. J. Verma, K. Hourigan, M. C. Thompson, W. Shen and P. P. Chan, *Adv. Healthc. Mater.*, 2015, **4**, 77-86.
25. R. K. Vadivelu, C. H. Ooi, R.-Q. Yao, J. Tello Velasquez, E. Pastrana, J. Diaz-Nido, F. Lim, J. A. K. Ekberg, N.-T. Nguyen and J. A. St John, *Sci. Rep.*, 2015, **5**, 15083.
26. J. Tian, N. Fu, X. D. Chen and W. Shen, *Colloids Surf. B*, 2013, **106**, 187-190.
27. T. Arbatan, L. Li, J. Tian and W. Shen, *Adv Healthc Mater*, 2012, **1**, 80-83.
28. R. K. Vadivelu, H. Kamble, A. Munaz and N. T. Nguyen, *Biomed. Microdevices*, 2017, **19**, 31.
29. T. Supakar, A. Kumar and J. O. Marston, *Phys. Rev. E Stat. Nonlin. Soft Matter Phys.*, 2017, **95**, 013106.
30. C. Planchette, A. L. Biance and E. Lorenceau, *EPL (Europhysics Letters)*, 2012, **97**, 14003.
31. E. Bormashenko, *Soft Matter*, 2012, **8**, 11018.
32. N. Eshtiaghi, J. S. Liu, W. Shen and K. P. Hapgood, *Powder Technol.*, 2009, **196**, 126-132.
33. J. Eggers, J. R. Lister and H. A. Stone, *JFM*, 1999, **401**, 293-310.
34. L. Duchemin, J. Eggers and C. Josserand, *JFM*, 2003, **487**, 167-178.
35. M. Wu, T. Cubaud and C.-M. Ho, *PhFl*, 2004, **16**, L51-L54.
36. D. G. Aarts, H. N. Lekkerkerker, H. Guo, G. H. Wegdam and D. Bonn, *Phys. Rev. Lett.*, 2005, **95**, 164503.
37. A. Menchaca-Rocha, A. Martinez-Davalos, R. Nunez, S. Popinet and S. Zaleski, *Phys. Rev. E Stat. Nonlin. Soft Matter Phys.*, 2001, **63**, 046309.